Neural oscillation as a selective modulatory mechanism on decision confidence, speed and accuracy

Amin Azimi[1], KongFatt Wong-Lin[1]

[1]Intelligent Systems Research Centre, School of Computing, Engineering and Intelligent Systems, Ulster University, Magee campus, Derry~Londonderry, Northern Ireland, UK

Corresponding author: KongFatt Wong-Lin (k.wong-lin@ulster.ac.uk)

Abstract

Neural oscillations have been associated with decision-making processes, but their underlying network mechanisms remain unclear. This study investigates how neural oscillations influence decision network models of competing cortical columns with varying intrinsic and emergent timescales. Our findings reveal that decision networks with faster excitatory than inhibitory synapses are more susceptible to oscillatory modulations. Higher in-phase oscillation amplitude reduces decision confidence without affecting accuracy, while decision speed increases. In contrast, anti-phase modulation increases decision accuracy, confidence and speed. Increasing oscillation frequency reverses these effects. Changing oscillatory phase difference gradually modulates decision behaviour, with decision confidence affected nonlinearly. These effects decouple decision accuracy, speed and confidence, challenge standard speed-accuracy trade-off, and can be explained via state-space trajectories' momentum swinging with respect to network steady states and decision uncertainty manifold. Our work provides mechanistic insights into how neurobiological diversity shapes decision-making processes in the presence of ubiquitous neural oscillations.

Introduction

Decision-making is a fundamental cognitive process involving the evaluation of options[1]. A prevalent phenomenon of decision-making is the speed-accuracy trade-off (Fig. 1a), where faster decisions are made at the expense of decision accuracy, while more accurate decisions more likely take longer time to be made[2,3]. Further, decision confidence, a type of metacognition, generally tends to be higher with quicker decisions[4] or higher decision accuracy (Fig. 1a)[5].

Decision making, and more generally, cognition, must be made amidst ongoing and ubiquitous neural oscillations—coherent fluctuations across frequency bands that coordinate neural activity[6]. In fact, a key component of processing neuroimaging data in cognitive neuroscience involves the handling of such frequency bands to identify neural correlate for specific cognition[7]. In particular, different oscillatory frequency bands have been suggested to be associated with distinct functions. For example, beta-band oscillations ($13-30\ Hz$) are linked to motor planning and decision-making[8,9] while gamma-band oscillations ($30-100\ Hz$) to attention, working memory and decision-making[10,11]. Specifically, neural oscillations are crucial for integrating sensory input with motor actions, allowing adaptive cognitive state transitions[12,13]. They shape decision-making by modulating neural communication timing and efficiency[6,14], with phase synchronization enhancing information transmission speed and reliability[10,15].

Non-invasive neuroimaging studies show that neural oscillations in gamma and beta bands predict perceptual decisions[16–18]. For example, Wimmer et al.[19] demonstrated that multiband oscillatory transitions in prefrontal circuits drive memory-guided decisions. Additionally, in visual discrimination tasks, alpha-band oscillations ($8-13\ Hz$) modulate

decision confidence without changing detection accuracy[20,21]. This implies that alpha oscillations might regulate the flow of sensory evidence during the decision-making process[22].

Decision making often involves multiple brain regions and timescales[23,24]. Moreover, sensory evidence accumulation timescale can vary across the cortex, which could be due to inherent differences in synaptic time constants[25] or network emergent phenomenon[24] across the cortical hierarchy. Understanding how these differential dynamics coordinate or modulate cognition in the presence of spontaneous neural oscillations is essential for comprehending their neural underpinnings in more realistic setting. Importantly, the computational neural circuit mechanisms of how neural oscillations influence decision-making are not well understood[26–28].

In this computational study, we address the above by first developing a canonical cortical column based neural circuit model for decision making extended from previous models[29,30]. Our model comprises two excitatory neural populations and one inhibitory neural population in each cortical column, with generated output encoding a potential decision outcome. When two cortical columns are coupled, the model can exhibit multistability that supports two-choice decision-making[31]. We considered two networks with different sets of synaptic time constants: one with faster excitatory than inhibitory synapses and another with slower excitatory than inhibitory synapses. We simulate spontaneous or background neural oscillations as inputs to the neural circuit models. This approach allowed us to systematically evaluate how spontaneous network oscillations affect decision circuit endowed with different synaptic timescales. We first replicate experimental findings from relevant previous studies and then made various model

predictions by varying the phases, amplitudes and frequencies of the neural oscillations. Our key findings are that neural oscillations can act as a novel and selective modulatory mechanism that can not only influence certain neural circuit type more but also can disentangle the tight relationship between decision speed, accuracy and confidence. We also provide dynamical systems analysis to explain these simulated phenomena. Overall, our study highlights the intricate interplay between neural oscillations and intrinsic neurobiological timescales in modulating decision dynamics.

Results

Decision networks operating at different timescales

Two-column cortical model for two-alternative decision-making endowed with neurophysiologically informed synaptic timescales and multistable dynamics was developed, building on our previous fully self-feedback neural mass model[29]. Each column comprised two excitatory neural populations and one inhibitory neural population (Fig. 1b; see Fig. S1 for details), each with self-feedback connectivity. Additionally, stimulus inputs were applied to the inhibitory population and an excitatory (e_1) population in both columns, consistent with previous studies[32,33]. Due to cross-columnar inhibition (Figs. 1b and S1), the model exhibited winner-take-all behaviour between the competing columnar neural population activities. Further, self-feedback allowed persistent activities for storage of decision made over time.

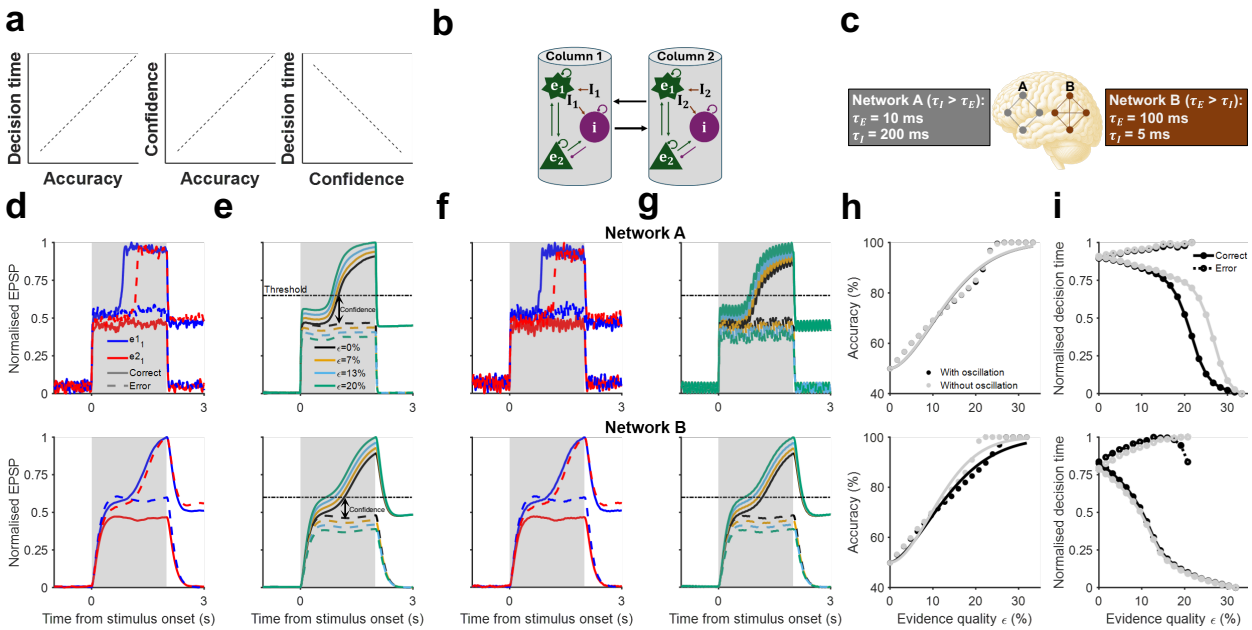

Fig. 1. Models exhibit stereotypical choice behaviour in two-choice reaction time tasks. **a** Illustration of well-known trade-offs between decision accuracy, time and confidence. **b** Schematic of two-column cortical neural mass model for 2-choice decision-making. **c** Models incorporate neurophysiologically plausible synaptic time constants (network A with excitatory synaptic time constant (τ_E) faster than that of inhibitory synapses (τ_I); network B: $\tau_E > \tau_I$). **d-i** Networks A (top) and B (bottom). **d** Sample single-trial simulation of normalised EPSP of neural populations e_1. Blue (red): correct (error) trials. Grey region: stimulus presence. $e1_1$: EPSP of neuron e_1 in column 1; $e2_1$: EPSP of neuron e_1 in column 2. **e** Normalised EPSP averaged over correct trials for different evidence qualities ϵ. Arrow: Decision confidence as the difference between output of winning column and losing column upon crossing decision threshold. **f** Simulated trials in the presence of oscillatory input (amplitude = 0.07 mA, frequency = 12 Hz). Solid (dotted): correct (error) trials. **g** Normalized EPSPs averaged over correct trials for different ϵ under oscillatory conditions. **h-i** Grey (black): with (without) oscillatory input. **h** Psychometric functions: decision accuracies vs. ϵ. **i** Chronometric functions: decision times vs. ϵ.

We further developed the above model into two types, A and B, each with different timescales characterised by different sets of synaptic time constants[34]. Specifically,

network A was presumed to be dominated by faster (e.g. AMPA-mediated) excitatory than (e.g. $GABA_B$-mediated) inhibitory synapses, while network B was dominated by slower (e.g. NMDA-mediated) excitatory than inhibitory (e.g. $GABA_A$-mediated) synapses[35] (Fig. 1c) (see Methods). The values of the synaptic time constants were selected based on known physiological ranges[35].

Upon stimulus presentation, both networks can produce distinct unitary choice outcomes with increasing activity for one of the excitatory neural populations (Figs. 1b and S1, populations e_1) in either competing cortical columns. Specifically, these circuits indicate a choice by having a columnar neural population's excitatory postsynaptic potential (EPSP) to ramp up over time towards a prescribed decision threshold, akin to temporal integration of evidence prior to choice commitment (Fig. 1d). The decision time was defined as the time from stimulus onset to decision threshold crossing of the "winning" neural population, and decision speed is inversely linked to this time. The confidence associated with the decision was computed at the decision time based on the difference between the activities of the winning column and the losing column which did not cross the threshold[36,37] (Fig. 1e). Further, the EPSP of the winning excitatory population increased more rapidly with higher evidence quality ε (indicating easiness level of task, e.g. equivalent to motion coherence in standard random-dot kinetogram[38]; see Methods) (Fig. 1e).

Motivated by a previous experimental study[21] which has identified the relationship between alpha oscillation ($8-13\,Hz$) with (perceptual) decision confidence, we first applied oscillatory input of $12\,Hz$ ($0.07\,mA$) on both networks A and B. We found that introducing $12\,Hz$ neural oscillations preserved the core decision-making and working

memory behaviours of the network models (Fig. 1f, g). Simulated trials in which a clear separation between the columnar EPSPs (difference of at least $0.01\,mV$ for network A; $0.08\,mV$ for network B) failed to occur are deemed invalid and excluded from consideration for both the psychometric and chronometric functions; this occurred only for about 5% for networks A and B in the study.

As evidence quality increased, the models' choice accuracy monotonically increased from chance level (50%) towards 100% (Fig. 1h; black line), while decision time decreased, with slower incorrect than correct choices (Fig.1i; black line), in agreement with stereotypical choice behaviour[1,39]. Additionally, persistent EPSP activity of the winning neural population after stimulus offset allowed for choice readout even after significant time delay by invoking working memory to store the decision made, consistent with previous studies[27,30,40–42]. Notably, our study demonstrates that network with faster excitatory than inhibitory synapses could still exhibit decision-making behaviour, challenging previous neurobiologically realistic computational modelling studies[27,30,42]. Interestingly, the initial rise time of such network's competing activities was rapid prior to their splitting[49–51]. Furthermore, applying $12\,Hz$ neural oscillations could alter the psychometric and chronometric functions (Fig. 1h, i; grey line), with decision accuracy being more resilient to neural oscillatory modulation. This hinted that neural oscillation might potentially disentangle decision's speed–accuracy trade-off[2,3], which we shall demonstrate with further evidence below.

In-phase oscillation amplitude distinctly affects decision networks with different timescales

As previous experimental studies have shown that neural oscillations in the alpha frequency band ($8 - 13\ Hz$) could influence perceptual decisions[20], we first applied in-phase sinusoidal modulation at a frequency of $12\ Hz$ to both cortical columns in both networks, simulating influence from spontaneous neural oscillations (Fig. 2a, $\epsilon = 7\%$). To compare the changes in decision time and confidence after modulation of oscillatory input, their values were normalised to their maximum values. For network A which had faster excitatory than inhibitory synapses, the $12\ Hz$ in-phase oscillatory modulation did not affect decision accuracy (Fig. 2b, dark grey) but decision confidence could be reduced by as much as about 15% (Fig. 2d, dark grey) for correct ($r = -0.89, p = 3.1 \times 10^{-8}$, Pearson correlation) and error trials ($r = -0.86, p = 4.2 \times 10^{-7}$). This was consistent with experimental findings that associate alpha oscillations with decreased confidence[20,22] in both correct and error trials while not affecting decision accuracy[20,22]. Additionally, decision time was predicted to be shortened by as much as about 5% for correct ($r = -0.90, p = 2.1 \times 10^{-8}$) trials (Fig. 2c, dark grey) and it shows no significant change for error trials.

For network B which had slower excitatory than inhibitory synapses, decision accuracy remained unchanged across varying oscillation amplitudes (Fig. 2b, brown), indicating that in-phase oscillatory activity did not affect the correctness of decisions made by the network. Additionally, increasing the oscillation amplitude did not significantly affect the decision times for either correct or error trials (Fig. 2c; brown). Moreover, there were no considerable changes in decision confidence observed in network B for both correct and error trials across different oscillation amplitudes (Fig. 2d; brown). This indicated that, at $12\ Hz$ oscillation frequency, increasing the oscillation amplitude did not affect decision

accuracy, time, or confidence for network B. In contrast, for network B, although $12\ Hz$ oscillation did not alter decision accuracy it reduced decision time and confidence

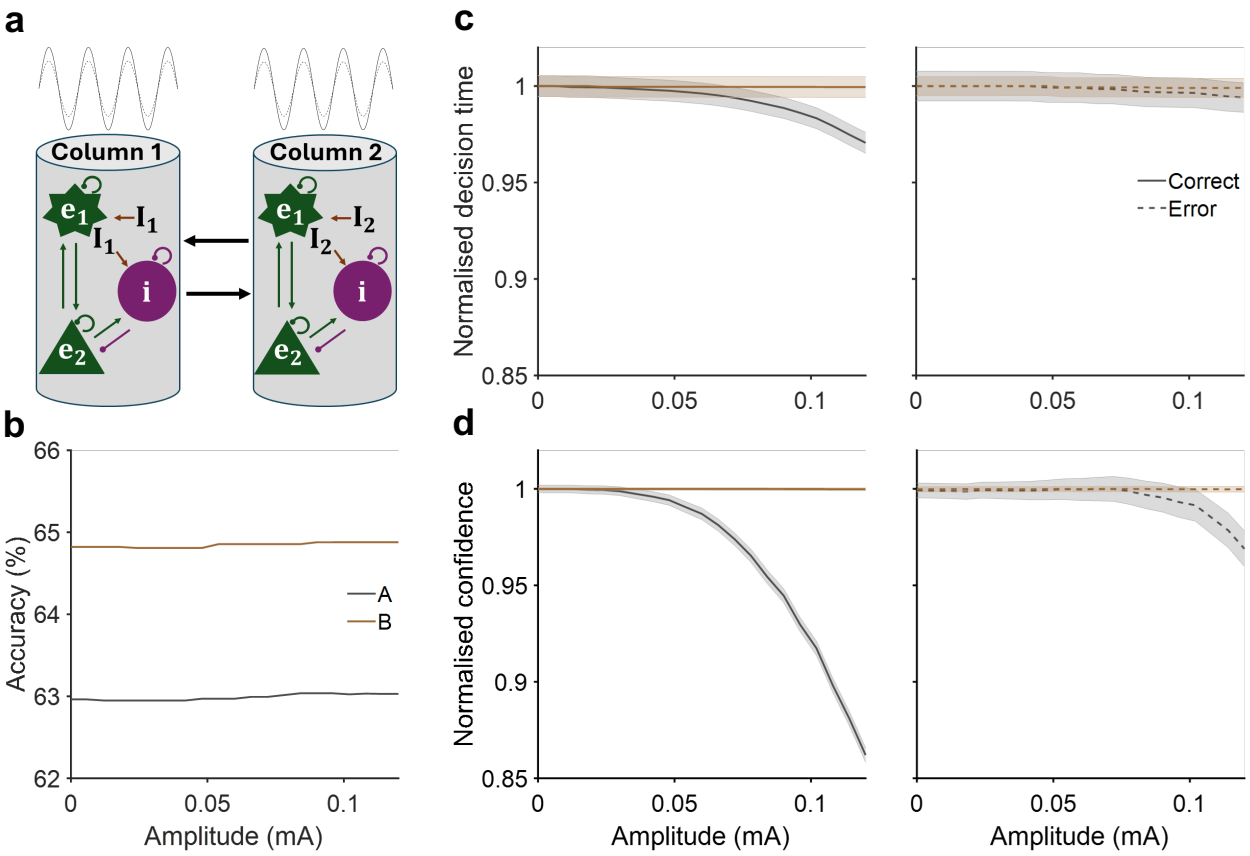

Fig. 2. Different effects of in-phase $12\ Hz$ neural oscillatory amplitude on networks with different timescales. **a** In-phase sinusoidal modulation at different amplitudes applied to both cortical columns for each network. **b** Decision accuracy remained unchanged for both networks. **c** For network A (grey), normalised decision time decreased with increasing oscillation amplitude for both correct (left) and error (right) trials; network B (brown) showed no significant changes in normalised decision time for both trial types. **d** For network A, normalised decision confidence decreased with higher oscillation amplitudes; network B showed no significant changes for both correct (left) and error (right) trials.

In-phase oscillation frequency effects are opposite that of amplitude modulation

Next, we investigate the effects of $12\ Hz$ neural oscillation frequency on decision-making behaviour by gradually increasing the input frequency to both networks A and B (Fig. 3a, amplitude=$0.08\ mA$). Our results indicated that higher frequencies did not noticeably alter decision accuracy in either network (Fig. 3b). Further, increasing the frequency did not significantly alter either decision time or confidence in network B across both trial types (Fig. 3c–d). In contrast, in network A (Fig. 3c–d), decision confidence increased by approximately 5% ($r = 0.69, p = 1.1 \times 10^{-3}$) and decision time by about 1% ($r = 0.75, p = 2.1 \times 10^{-4}$) for correct trials, with no significant changes observed for error trials. These findings demonstrate that the alpha frequency range for network A may be optimal for influencing both decision time and confidence while maintaining accuracy.

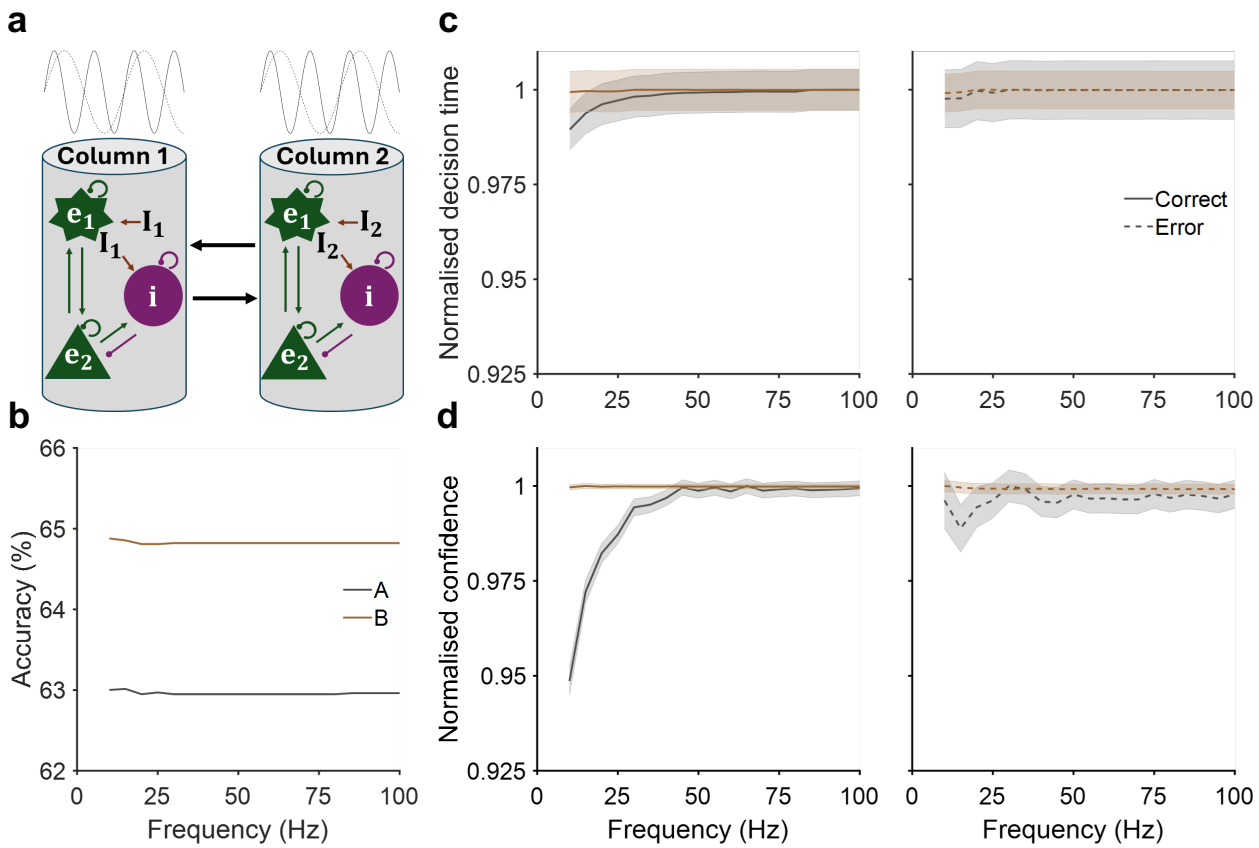

Fig. 3. Different effects of in-phase neural oscillatory frequency (amplitude = $0.08\ mA$) on networks with different timescales. **a** In-phase sinusoidal modulation at different frequencies applied to both cortical columns for each network. **b** Decision accuracy remained unchanged for both networks. **c**, **d** For Network A, normalized decision time (c, grey) and confidence (d) increased for correct trials (left) but showed no substantial change for error trials (right). In contrast, for Network B, neither decision time nor confidence changed significantly for either type of trial (c–d, brown).

Anti-phase oscillation amplitude enhances decision efficiency

Neural oscillation may not necessarily have to affect different brain locations synchronously. For instance, this may be due to transduction or conduction delays in receiving neural signals[43]. Hence, we next examine the other extreme case of neural oscillations with anti-phase sinusoidal modulation between the two competing cortical

columns. We began by applying oscillatory modulation at a frequency of $12\,Hz$ (alpha band) to both cortical columns within each network (Fig. 4a, grey). For network A, enhancing the amplitude of anti-phase oscillatory modulation led to improved decision accuracy (by ~40%) (Fig. 4b, dark grey, $r = 0.98$, $p = 1.2 \times 10^{-15}$), decreased decision time (by ~40%) for correct trials ($r = -0.99$, $p = 1.0 \times 10^{-21}$), and slight increase of decision time (by ~10%) for error trials (Fig. 4c, dark grey, $r = 0.84$, $p = 1.8 \times 10^{-6}$). Additionally, decision confidence increased for both trial types (Fig. 4d, dark grey, $r = 0.92$, $p = 2.2 \times 10^{-9}$ for correct, $r = 0.64$, $p = 2.0 \times 10^{-3}$ for error). This suggests that anti-phase oscillations can facilitate more accurate and faster decisions, unlike standard speed-accuracy trade-off mechanisms.

For network B, increasing the amplitude of anti-phase oscillatory modulation resulted in enhanced decision accuracy (by ~40%) (Fig. 4b, brown, $r = 0.88$, $p = 1.5 \times 10^{-7}$), decreased decision time for correct trials (by ~40%) ($r = -0.99$, $p = 1.0 \times 10^{-21}$) and increased decision time for error trials (by ~20%) ($r = 0.85$, $p = 1.4 \times 10^{-6}$), and stable decision confidence across both trial types. The slower error decisions led to further temporal accumulation of evidence and enhancing evidence quality. Thus, this suggests that anti-phase neural oscillations can make more efficient decisions without overly affecting decision confidence, regardless of the network's timescale.

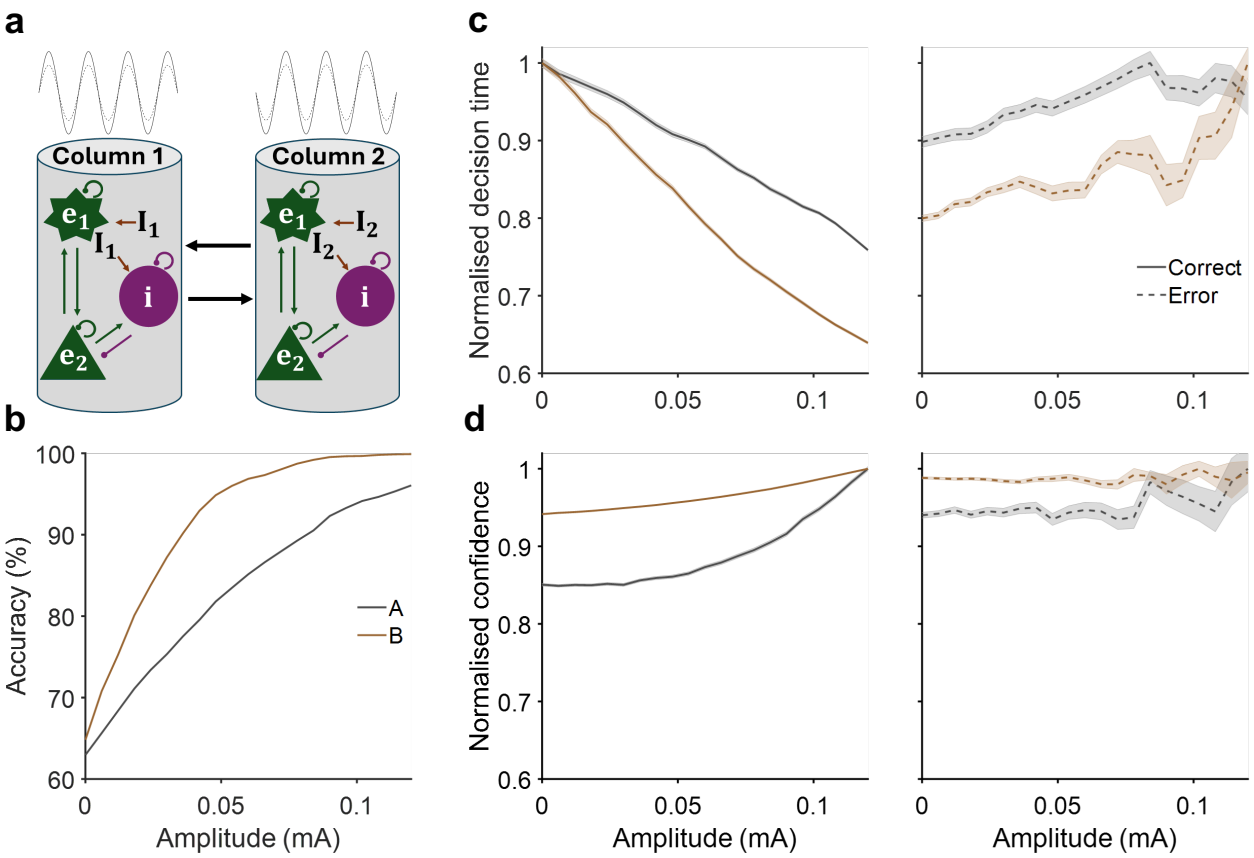

Fig. 4. Anti-phase $12\ Hz$ neural oscillatory amplitude enhances decision accuracy and modulates decision speed. **a** Anti-phase sinusoidal modulation with varying amplitudes applied to both cortical columns for each network. **b** Decision accuracy improved with higher oscillation amplitudes in both networks. **C** Normalised decision time decreased with increasing amplitude for correct trials (left), while increasing for error trials (right). **d** Normalized decision confidence increased in Network A for both correct and error trials, as well as for correct trials in Network B. However, no substantial change was observed in Network B for error trials.

Anti-phase oscillation frequency effects are opposite that of amplitude modulation

As in the in-phase oscillation modulation investigation, here we increased the frequency of anti-phase oscillatory modulation and observed longer decision time for correct trials (amplitude = $0.08\ mA$, $r = 0.80$, $p = 4.0 \times 10^{-5}$ for network A; $r = 0.84$, $p = 6.5 \times 10^{-6}$ for network B), shorter decision times for error trials ($r = -0.51$, $p = 0.03$ for network A;

$r = -0.84$, $p = 7.30 \times 10^{-6}$ for network B), and decreased decision accuracy ($r = -0.84$, $p = 6.6 \times 10^{-6}$ for network A; $r = -0.91$, $p = 4.4 \times 10^{-8}$ for network B), while decision confidence decreased for correct trials in both networks ($r = -0.77$, $p = 1.2 \times 10^{-4}$ for network A, $r = -0.73$, $p = 4.3 \times 10^{-4}$ for network B) and did not change significantly for error trials in either network (Fig. 5d). These results suggest that, in contrast to anti-phase amplitude modulation, anti-phase frequency modulation exhibited the opposite trend for both network types (enhanced decision accuracy, prolonged correct decision times, shortened error decision times).

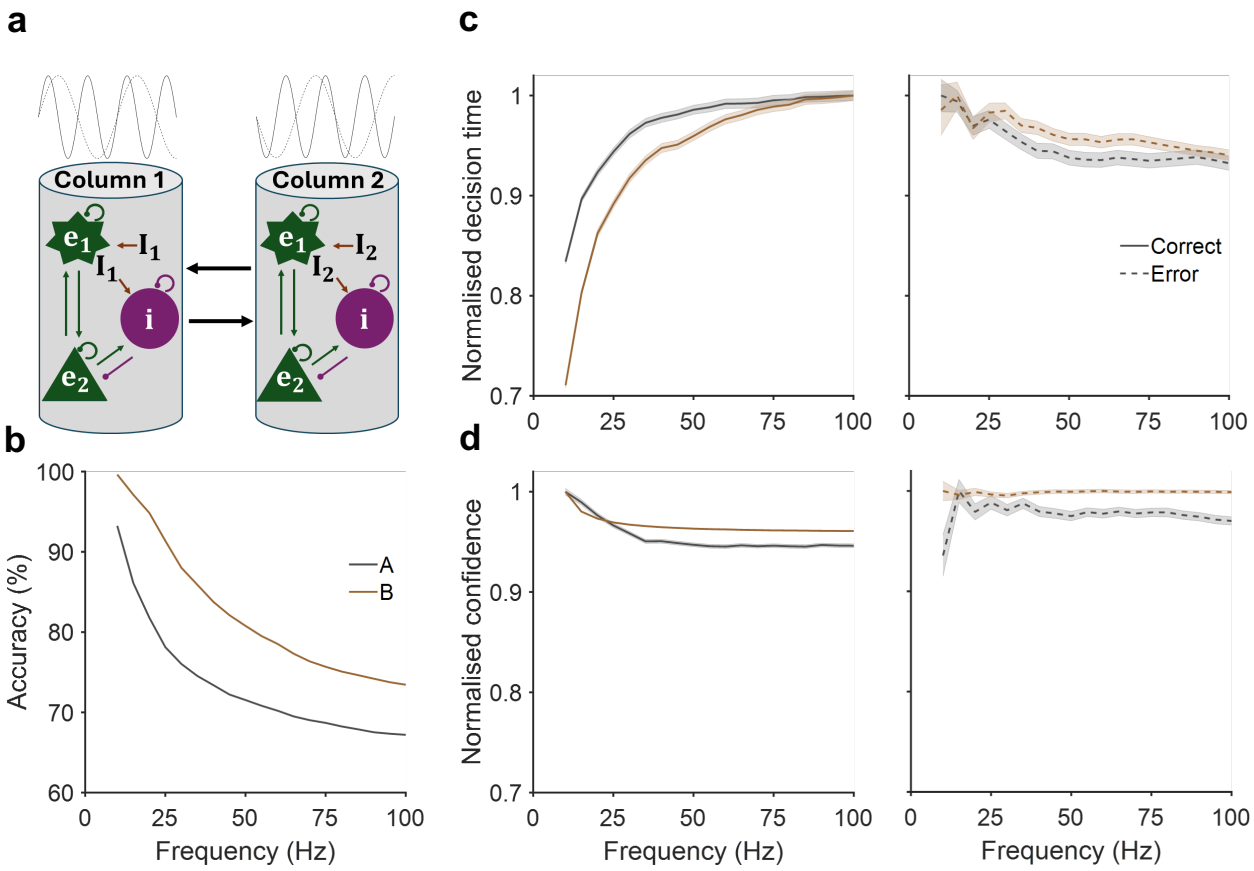

Fig. 5 The effects of anti-phase neural oscillatory frequency (amplitude = $0.08\ mA$) are the opposite of those of amplitude oscillation. **a** Anti-phase sinusoidal modulation with varying frequencies applied to both cortical columns for each network. **b** Decision accuracy declined with higher oscillation frequencies in both networks. **c** Normalised decision time increased with increasing amplitude for correct trials (left), while it

decreased for error trials (right). **d** Normalised decision confidence decreased for correct trials in both networks, and showed no substantial change for error trials.

Oscillatory phase difference progressively affects decision behaviours

We investigated how gradual changes in oscillatory phase differences ($\Delta\phi$) between neural inputs affect decision-making in ~~two~~ networks A and B. Building on prior analyses of in-phase and anti-phase effects, we adjusted $\Delta\phi$ between inputs to network A, with the phase to column 1 (encoding correct decision) leading that of column 2 (encoding error decision) (Fig. S2).

In network A, decision accuracy increased sharply at larger phase differences (e.g., $\Delta\phi = \pi$) compared to smaller ones (e.g., $\Delta\phi = 0$), especially as oscillatory amplitude increased (Fig. S2a). Conversely, decision time decreased more rapidly at larger $\Delta\phi$ (Fig. S2b). Interestingly, as phase difference increased, decision confidence changed from decreasing to increasing trends with oscillation amplitude (Fig. S2c). Network B exhibited similar trends for decision accuracy and decision time, but decision confidence only (slightly) increased with oscillation amplitude (Fig. S2d–f).

When the oscillatory input to column 2 (error decision) led column 1 (correct decision), network A exhibited a decline in decision accuracy as amplitude increased at larger $\Delta\phi$ (Fig. S3a). As the phase difference increased, decision time and decision confidence (**c**) changed from decreasing to increasing trends with oscillation amplitude (Fig. S3b–c). For network B, increasing $\Delta\phi$ led to decreased decision accuracy as in network A, but decision time only increased with oscillation amplitude while decision confidence stayed largely constant (Fig. S3d–f).

After reversing the phase lead between columns 1 and 2, for network A, as $\Delta\phi$ increased, decision accuracy progressively increased but with decreasing trend with oscillation frequency (Fig. S4a), while decision time decreased but with increasing trend with oscillation frequency (Fig. S4b). The decision confidence changed from increasing to decreasing trends with oscillation frequency (Fig. S4c). For network B, decision accuracy and decision time exhibited similar trends as in network A, but decision confidence only slightly decreased with oscillation frequency (Fig. S4e–f).

With the input to column 2 leading again, increasing $\Delta\phi$ led to decision accuracy progressively decreasing with increasing trend with oscillation frequency (Fig. S5a), and decision time decreased with oscillation frequency (Fig. S5b), while decision confidence changed from increasing to decreasing trends with oscillation frequency (Fig. 5c). For network B, the trends are similar except that decision confidence did not significantly change with oscillation frequency or phase difference (Fig. S5c, f).

Overall, we have shown that where the oscillatory phase lead resided, in neural population encoding correct or error decision, can have decision network be differently modulated by phase difference and oscillation amplitude or frequency. The non-monotonic effects on decision confidence deserve further discussion. Specifically, as the model's decision confidence is defined as the difference between the winning and losing population's EPSP activities at the moment of decision threshold crossing, and given that network A is more sensitive to oscillatory influences than network B, when the phase difference between the oscillatory inputs to both columns is closer to π, the difference between the winner and loser EPSP activities reached its maximum value, whereas at a phase difference closer to 0, this difference reached its minimum value. Moreover,

depending on the interplay between stimulus input, noise and intrinsic network dynamics, the decision confidence trends of network A could reverse. Thus, our simulation results highlight the intricate role of phase relationships in neural oscillatory modulations on decision-making.

Mechanistic insights into oscillation-induced decision modulation

Next, we seek to understand the mechanisms underlying the above simulated results. Given that phase differences generally affect decision behaviours in a progressive manner, it suffices to provide a conceptual understanding for the two extreme cases: in-phase and anti-phase neural oscillatory modulations. This can be investigated by projecting the trial-averaged trajectories onto lower (two) dimensional state (decision) space. For simplicity, we focused only with stimulus bias of 7%.

Our simulations generally indicated that, for network A, in-phase modulation of neural oscillation with higher amplitudes tended to retain the network state along the decision uncertainty manifold (i.e., along the state-space diagonal) in state space (Fig. 6a), hence, decreasing decision confidence. Concurrently, larger oscillation amplitudes led to larger deflection in phase space, leading to greater momentum towards the choice attractors without favouring any of the choices. Therefore, these explain why for network A, in-phase amplitude-modulation decreased decision confidence while expediting decision formation, without influencing decision accuracy (Fig. 2).

Conversely, anti-phase neural oscillation with higher amplitudes provided swinging momentum towards the choice attractors for network A, with a greater tendency for correct choices (Fig. 6b), and leading to more accurate decisions. Further, higher oscillatory amplitude exerted a greater tendency to move the network state (orthogonally)

away from the decision uncertainty manifold, increasing decision confidence. Although one might consider anti-phase modulation with higher oscillation amplitude to also deflect trajectories more in state space, for error choices, the network state also passed closer towards a metastable saddle steady state (Fig. 6b), which in turn slowed trajectories[30,44] and leading to slower error decision times. Therefore, these explain why for network A, anti-phase amplitude-modulation increased decision accuracy and confidence, and expedited decision formation for correct trials while slowing error trials (Fig. 4).

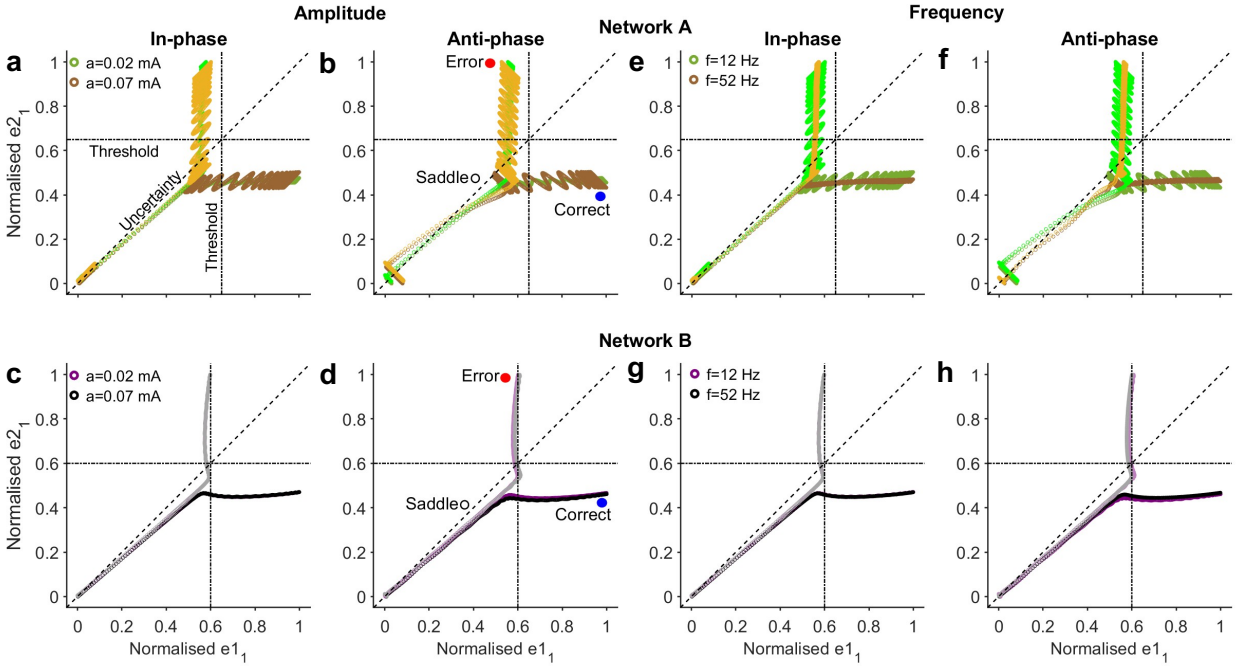

Fig. 6. Neural oscillations on choice behaviour in (projected) state space. In state (EPSP) space, the trajectories denote neural population EPSPs ($e1_1$ and $e2_1$), averaged across correct or error trials (with 7% stimulus bias). Top: Network A. Higher amplitude/frequency, brown (gold) trajectories indicate correct (error) trials; lower amplitude/frequency, dark (light) green for correct (error) trials. Bottom: Network B. Higher amplitude/frequency, dark (light) grey trajectories indicate correct (error) trials; lower amplitude/frequency, dark (light) purple for correct (error) trials. **a-d** Modulation due to in-phase (**a, c**) and anti-phase (**b, d**) with different oscillation amplitudes. **e-h** Modulation due to in-phase (**e, g**) and anti-phase (**f, h**) with different oscillation frequencies. Filled (unfilled) circle: stable choice attractor (metastable saddle-

like steady state); blue (red) for correct (error) choice. Although indicated only in (**b**) and (**d**), they exist, in the same positions, in other panels (not indicated for clarity). Time spacing between consecutive trajectory points for network A (B) is 1 ms (5 ms).

For network B, in-phase oscillatory modulatory effects were less prominent with higher oscillation amplitude (Fig. 6c) due to the slow excitatory synapses filtering out oscillatory inputs, making the network more robust to such perturbations (Fig. 2). However, with anti-phase oscillatory modulation, larger oscillation amplitude increased the tendency to slightly move towards the correct attractor faster but slower for the error attractor, while also moving away from the uncertainty manifold (Fig. 6d). Thus, for network B, anti-phase modulation with increasing amplitude increased decision accuracy and confidence while expediting decision formation for correct trials and slowing error trials (Fig. 4).

In terms of in-phase oscillation with varying frequency, network A's state tended to remain along the decision uncertainty manifold in state space at lower frequencies and slower towards choice attractors without biasing towards a specific attractor (Fig. 6e). Therefore, with network A, in-phase modulation with increasing frequency increased decision confidence while slowing decision formation, without influencing decision accuracy for network A (Fig. 3).

In contrast, albeit non-intuitively, anti-phase neural oscillation with lower frequency manifested as if they had larger trial-averaged trajectory fluctuations akin to larger oscillation amplitudes (compared with Figs. 6a-b). Hence, the explanations of the simulated behaviour were reverse of that with higher oscillation amplitude (see above). Thus, for network A, anti-phase oscillatory modulation with increased frequency decreased decision accuracy and confidence while increasing decision time (Fig. 5).

For network B, in-phase oscillatory modulation was not noticeable with increasing frequency (Fig. 6g), explaining the simulated results in Fig. 3. However, for anti-phase oscillatory modulation with increasing oscillation frequency, it had the opposite, albeit subtle, effect as with increasing oscillation amplitude (compare Fig. 6h with Fig. 6d). This explained the reverse trends observed in Fig. 5.

Discussion

In this study, we developed a cortical-column decision network model comprising multiple neural populations with self-feedback to investigate the computational mechanisms underlying the influence of neural oscillations on perceptual decision-making. By simulating two-alternative forced-choice tasks with networks exhibiting different synaptic time constants (network A: $\tau_I > \tau_E$; network B: $\tau_E > \tau_I$), and hence different emergent network dynamics, we explored how in-phase and anti-phase sinusoidal modulations at various frequencies and amplitudes affect decision accuracy, speed and confidence. It should be noted that this computational study was synaptic specific agnostic but focuses generally on the effects of neural oscillation on these two extreme combinations of excitatory and inhibitory synaptic dynamics. Our findings reveal that neural oscillations can selectively modulate decision confidence and speed without altering accuracy, and can also violate the standard decision speed-accuracy trade-off relationship[2,3]. Importantly, these effects are contingent on the synaptic composition of the underlying neural circuits.

Consistent with previous empirical studies[20,22], we found that in-phase sinusoidal modulation at 12 Hz (alpha band) did not affect decision accuracy but significantly

reduced decision confidence in network A (Figs. 2 and 3). This aligns with existing findings that alpha oscillations modulate decision confidence but not decision accuracy[20,22]. Particularly, at least for the oscillation amplitude investigated, the alpha frequency laid within the lower frequency range where the modulatory effects were the largest (Fig. 3). These results support the notion that lower frequency neural oscillations, including the alpha band, may play a crucial role in regulating the flow of sensory information for decision-making[12,13].

Compared to in-phase modulations, our simulations demonstrated that anti-phase oscillatory modulations reveal different effects. Specifically, anti-phase modulation with increasing oscillation amplitude decreased decision time but increased decision accuracy and confidence (Figs. 4). These effects were reversed if oscillation frequency was increased instead (Fig. 5). These suggest that anti-phase oscillations may facilitate more efficient decisions, while clearly violating standard speed-accuracy trade-off[2,3].

Neural oscillations were generally found to be more selective to network A than network B (Figs. 1-5). For in-phase oscillatory modulations, network B's slow excitatory dynamics filtered out the oscillatory perturbations (Figs. 1f-i and 6) such that there were negligible oscillatory effects, unlike for network A (Figs. 2 and 3). For anti-phase oscillatory modulations, both were modulated with similar trends albeit lesser effects for network B (Figs. 4 and 5). These highlight the importance of the underlying synaptic time constants in shaping the influence of neural oscillations on cognitive functions.

Although we have selected synaptic time constant values in this study to be within physiological ranges, we found our results to hold using other values (not shown). That is, decision networks with faster excitatory, or slower inhibitory synaptic dynamics, are

more susceptible to oscillation-induced modulation, which aligns with the understanding that inhibitory neurons play a critical role in controlling the timing and synchrony of neural activity[45], and that variations in synaptic time constants can influence the integration of sensory information over time[23,24]. Interestingly, there is evidence of variability in decision and synaptic timescales across the brain[24,25]. Our study predicts that some of these local neural circuits will be more influenced by neural oscillations than others.

Between the extreme in-phase and anti-phase cases, we also investigated how gradual change in phase difference affects decision behaviours (Figs. S2-5). We found that it matters which specific neural population leads the oscillatory phase. When the oscillatory phase is led by the neural population which encodes correct decision, decision accuracy can increase while decision becomes faster, allowing more efficient decisions while violating speed-accuracy trade-off. The present findings underscore the critical role of oscillation phase relationships in shaping decision dynamics[15,46].

To facilitate the explanation of the decision networks' simulated behaviours under various neural oscillatory amplitudes and frequencies, we projected the networks' trajectories in lower dimensional state or decision space. The sensitive influence on network A's trajectories and hence its decision behaviours could be clearly visualised (Fig. 6, top), as compared to the negligible or much smaller effects on network B, which robustly filtered out these perturbations (Fig. 6, bottom). Oscillatory effects on decision accuracy, confidence and speed could be largely accounted for by momentum swinging of network trajectories towards choice attractors and along/away from decision uncertainty manifold. Additionally, decision time was further influenced by the network trajectory's proximity to a metastable saddle-like steady states. Interestingly, increasing oscillation frequency

(Figs. 6e-h) had the opposite effect as increasing oscillation amplitude (Figs. 6a-d). Taken together, these provide a mechanistic framework in which phase-specific interactions of oscillatory inputs and synaptic integration actively sculpt decision processes—toggling between rapid but uncertain states under in-phase modulation and more decisive, confidence-enhancing states under anti-phase modulation.

Our findings extend previous computational models of decision-making by incorporating neural oscillations and synaptic time constant variability. Prior models have largely focused on drift-diffusion frameworks[47] or population-based (neural mass or mean-field) models without oscillatory inputs[30]. By introducing background oscillatory modulation, our model accounts for empirical observations where alpha-band oscillations modulate decision confidence without affecting accuracy[20,22]. Moreover, our model demonstrates that altering oscillation frequency and amplitude can modulate decision times independently of accuracy, providing a novel neural mechanism for disentangling decision speed, accuracy and confidence.

By accounting for the key characteristics of neural oscillations across different frequency bands and their influence on decision confidence and accuracy, our model bridges the gap between empirical observations and computational theories. This advancement opens new avenues for exploring novel neuromodulation and therapeutic interventions in clinical populations where decision-making dynamics are compromised while enhancing our understanding of the complexities of human cognition in the presence of ubiquitous neural oscillations.

While our work captures key aspects of how neural oscillations influence decision-making, it is based on several assumptions. First, we modelled oscillations as sinusoidal

inputs, whereas in the brain, oscillations are often irregular and interact across multiple frequencies[48]. Secondly, we only investigate a single (two-alternative) decision-making task. Moreover, we did not explicitly model the generation of neural oscillations. Thus, future work could include more realistic neural oscillatory dynamics, investigate under different decision task paradigms, and explore how chemical neuromodulators may interact with oscillations to influence decision-making. Furthermore, examining oscillatory dynamics in individuals with neurological disorders may reveal the underlying pathological mechanisms that disrupt decision-making processes and pave the way for targeted therapeutic interventions.

In summary, our study provides a novel computational framework that elucidates the neural circuit mechanisms by which neural oscillations modulate decision-making processes. By demonstrating that oscillatory inputs can decouple decision confidence, speed and accuracy beyond standard speed-accuracy trade-off, and that these effects depend on synaptic timescales, we bridge the gap between empirical findings and theoretical models. Our work highlights the intricate interplay of neural oscillations and synaptic dynamics in cognitive functions and opens new directions for investigation.

Methods

Cortical columnar neural mass model for decision-making

We develop a two-column cortical model for two-alternative decision-making based on our fully self-feedback neural mass model[29], The model comprises two excitatory neural populations (e_1 and e_2) and one inhibitory neural population (i) in each column. This model integrates inputs into both the excitatory and inhibitory populations, and incorporates

lateral interactions between the columns, as depicted in Fig. 1b (see Fig. S1 for details), allowing winner-take-all behaviour that is required for forming unitary decision.

Postsynaptic potential function

In this model, the function S, characterized by a sigmoidal shape, represents the postsynaptic potentials and is defined as:

$$S(v) = \frac{1}{1+\exp\left(-r_1(v-r_2)\right)} - \frac{1}{1+\exp(r_1 r_2)} \quad (1)$$

where r_1 $(= 2)$ and r_2 $(= 1)$ are parameters controlling the characteristics of the sigmoid function; increasing r_1 steepens the slope, while increasing r_2 shifts the curve to the right. The average membrane depolarisation v (or postsynaptic potentials) associated with a neural population serves as the presynaptic input for other connected neural populations, including other cortical columns, through the connections as described by $S(v)$[29]. The priors and physiological interpretations of the model parameters are provided in Table 1.

Model parameters

Table 1: Priors and physiological interpretations of model parameters. Subscript e (i) denote excitatory (inhibitory). Compare with Fig. S1.

Parameter	Physiological interpretation	Value
He, Hi	Excitatory and inhibitory magnitude in synaptic function	$3.25, 22\ [mV]$
$K_e = \frac{1}{\tau_e}$, $K_i = \frac{1}{\tau_i}$ (Network A)	Excitatory and inhibitory rate constant (AMPA, $GABA_B$)	$100, 2\ [s\ -1]$
$K_e = \frac{1}{\tau_e}$, $K_i = \frac{1}{\tau_i}$ (Network B)	Excitatory and inhibitory rate constant (NMDA, $GABA_A$)	$10, 100\ [s\ -1]$
c_1, c_2, c_3, c_4 (Network A)	Intrinsic coupling parameters for each column	$0.1, 0.1, 8, 5$
c_1, c_2, c_3, c_4 (Network B)	Intrinsic coupling parameters for each column	$0.15, 0.1, 32, 55$
c_5, c_6, c_7 (Network A)	Intrinsic coupling parameters in feedback loops for each column	$0.3, 1, 105$
c_5, c_6, c_7 (Network B)	Intrinsic coupling parameters in feedback loops for each column	$50, 0.1, 31.5$
c_{ee}, c_{ei}, c_{ee}' , c_{ei}' (Network A)	Extrinsic coupling parameters (lateral connections)	$0.7, 30, 0.7, 30$
c_{ee}, c_{ei}, c_{ee}' , c_{ei}' (Network B)	Extrinsic coupling parameters (lateral connections)	$0.85, 50, 0.85, 50$

Model equations

Fig. 1b (see Fig. S1 for details) illustrates that neural population e_2 in the first column is laterally connected to neurons e_1 in the second column, and vice versa. Additionally, there are lateral connections between neurons e_2 in the first column and neurons i in the second column, and vice versa. Accordingly, the dynamical equations describing the model can be described as follows (see Table 1 for notation meaning).

For cortical column j (the other column denoted as k):

Post-synaptic potential for $e1_j$:

$$\dot{v}1_j = y1_j \tag{2}$$

$$\dot{y}1_j = H_e K_e[c_1 \mathrm{S}(v2_j - v3_j + v7_j) + c_{ee}' \mathrm{S}(v9_k - v10_k + v14_k) + I_1] - 2K_e y1_j - K_e^2 v1_j \tag{3}$$

Post-synaptic potential for $e2_j$:

$$\dot{v}2_j = y2_j \tag{4}$$

$$\dot{y}2_j = H_e K_e[c_2 \mathrm{S}(v1_j + v6_j)] - 2K_e y2_j - K_e^2 v2_j \tag{5}$$

$$\dot{v}3_j = y3_j \tag{6}$$

$$\dot{y}3_j = H_i K_i[c_3 \mathrm{S}(v4_j - v5_j)] - 2K_i y3_j - K_i^2 v3_j \tag{7}$$

Post-synaptic potential for i_j:

$$\dot{v}4_j = y4_j \tag{8}$$

$$\dot{y}4_j = H_e K_e[c_4 \mathrm{S}(v2_j - v3_j + v7_j) + c_{ei}' \mathrm{S}(v9_k - v10_k + v14_k) + I_1] - 2K_e y4_j - K_e^2 v4_j \tag{9}$$

Post-synaptic potential due to self-inhibition for i_j:

$$\dot{v}5_j = y5_j \tag{10}$$

$$\dot{y}5_j = H_i K_i[c_5 \mathrm{S}(v4_j - v5_j)] - 2K_i y5_j - K_i^2 v5_j \tag{11}$$

Post-synaptic potential due to self-excitation for $e1_j$:

$$\dot{v}6_j = y6_j \tag{12}$$

$$\dot{y}6_j = H_e K_e[c_6 \mathrm{S}(v1_j + v6_j)] - 2K_e y6_j - K_e{}^2 v6_j \tag{13}$$

Post-synaptic potential due to self-excitation for $e2_j$:

$$\dot{v}7_j = y7_j \tag{14}$$

$$\dot{y}7_j = H_e K_e[c_7 \mathrm{S}(v2_j - v3_j + v7_j)] - 2K_e y7_j - K_e{}^2 v7_j \tag{15}$$

Model input

Then, we model the stimulus input to both columns using a Gaussian bump function[49]:

$$u_1(t) = (a + \Delta) * e^{\frac{-(t-t_0)^2}{\Delta t^2}} \tag{16}$$

$$u_2(t) = (a - \Delta) * e^{\frac{-(t-t_0)^2}{\Delta t^2}} \tag{17}$$

Here, a represents the amplitude for zero bias (Δ), t_0=1 s is the stimulus onset time, t=3 s is the stimulus offset time, and Δt (0.007 s) controls the width of the Gaussian bump. Additionally, we measure the evidence quality ε (analogous to motion coherence[38]) using the following definition:

$$\varepsilon = \frac{u_1(t_0) - u_2(t_0)}{u_1(t_0) + u_2(t_0)} \tag{18}$$

Also, noise is incorporated into the dynamics of the excitatory e_1 and inhibitory i populations via inputs I_η, processed through rapid synaptic activation mediated by AMPA receptors. The dynamics governing this interaction is described by[50]:

$$\frac{dI_\eta}{dt} = -\frac{I_{\eta 1}}{\tau_{\mathrm{AMPA}}} + \frac{\eta(t)}{\sqrt{\tau_{\mathrm{AMPA}}}} \tag{19}$$

Here, τ_{AMPA}= 5 ms, and I_η is a white Gaussian noise with zero mean and standard deviation of 0.02 nA.

In addition, background input (I_0) and sinusoidal stimulation (I_O) at a frequency f (12 Hz) are incorporated into the background noise of the inputs received by both cortical columns, mimicking spontaneous brain oscillations[51]. The total input current to each of the columns is therefore:

$$I(t) = u(t) + I_\eta(t) + I_O(t) \tag{20}$$

Model analysis

We numerically integrate the nonlinear equations of the model using the Euler-Maruyama method in MATLAB R2023b, with a temporal resolution of 1 ms. Simulations are conducted to investigate two-alternative decision-making and decision storage through multistable dynamics. We manipulate the intrinsic and lateral inhibitory and excitatory connections to examine the multistability of the postsynaptic potentials in e_1 as influenced by input currents, utilising XPPAUT 8.0 for these simulations[52].

Due to the symmetry of the cortical columns, we assume without loss of generality that activity in the first column encodes the correct choice. Specifically, we increase the input to the first column relative to the second column. We then classify the simulated trials into three categories: (1) correct trials, characterised by a significantly higher output from the first column; (2) error trials, identified by a higher output from the second column; and (3) non-decision trials, defined by an output difference that do not surpass a predefined threshold (network A: 0.01 mV; network B: 0.08 mV).

Statistical Analysis

Statistical analyses are performed using MATLAB R2023b. Correlations are calculated using Pearson correlation coefficient, with statistical significance set at $p < 0.05$.

Data and Code Availability

The simulations and figure generation for this study are conducted using MATLAB, and all the associated code will be made openly available upon publication. Since all data are generated through simulations of the model, no empirical data collection is necessary.

Author Contributions

A.A., K.W.-L. designed and conceptualised analyses. A.A. performed the analysis, modelling and statistical analyses. A.A. and K.W.-L. validated the analyses. A.A. and K.W.-L. wrote the paper. K.W.-L. supervised the research.

Funding

A.A. and K.W.-L. were supported by HSC R&D (STL/5540/19) and MRC (MC_PC_20020).

Competing Interests

The authors declare no competing interests.

References

1. Gold, J. I. & Shadlen, M. N. The neural basis of decision making. *Annu. Rev. Neurosci.* **30**, 535–574 (2007).
2. Heitz, R. P. The speed-accuracy tradeoff: history, physiology, methodology, and behavior. *Front. Neurosci.* **8**, 150 (2014).
3. Bogacz, R., Wagenmakers, E. J., Forstmann, B. U. & Nieuwenhuis, S. The neural basis of the speed–accuracy tradeoff. *Trends Neurosci.* **33**, 10–16 (2010).

4. Hellmann, S., Zehetleitner, M. & Rausch, M. Confidence Is Influenced by Evidence Accumulation Time in Dynamical Decision Models. *Comput. Brain Behav.* **7**, 287–313 (2024).

5. Jin, S., Verhaeghen, P. & Rahnev, D. Across-subject correlation between confidence and accuracy: A meta-analysis of the Confidence Database. *Psychon. Bull. Rev.* **29**, 1405–1413 (2022).

6. Fries, P. Rhythms for cognition: communication through coherence. *Neuron* **88**, 220–235 (2015).

7. Buzsáki, G. *Rhythms of the Brain*. xv, 448 (Oxford University Press, New York, NY, US, 2006). doi:10.1093/acprof:oso/9780195301069.001.0001.

8. Engel, A. K. & Fries, P. Beta-band oscillations—signalling the status quo? *Curr. Opin. Neurobiol.* **20**, 156–165 (2010).

9. Baker, A. P. *et al.* Fast transient networks in spontaneous human brain activity. *eLife* **3**, e01867 (2014).

10. Pesaran, B., Pezaris, J. S., Sahani, M., Mitra, P. P. & Andersen, R. A. Temporal structure in neuronal activity during working memory in macaque parietal cortex. *Nat. Neurosci.* **5**, 805–811 (2002).

11. Siegel, M., Donner, T. H. & Engel, A. K. Spectral fingerprints of large-scale neuronal interactions. *Nat. Rev. Neurosci.* **13**, 121–134 (2012).

12. Wang, X.-J. Neurophysiological and computational principles of cortical rhythms in cognition. *Physiol. Rev.* **90**, 1195–1268 (2010).

13. Wang, X.-J. Probabilistic decision making by slow reverberation in cortical circuits. *Neuron* **36**, 955–968 (2002).

14. Siegel, M., Engel, A. K. & Donner, T. H. Cortical network dynamics of perceptual decision-making in the human brain. *Front. Hum. Neurosci.* **5**, 21 (2011).

15. Buschman, T. J. & Miller, E. K. Top-down versus bottom-up control of attention in the prefrontal and posterior parietal cortices. *Science* **315**, 1860–1862 (2007).

16. Donner, T. H., Siegel, M., Fries, P. & Engel, A. K. Buildup of choice-predictive activity in human motor cortex during perceptual decision making. *Curr. Biol.* **19**, 1581–1585 (2009).

17. Benwell, C. S. *et al.* Prestimulus EEG power predicts conscious awareness but not objective visual performance. *eNeuro* **4**, ENEURO.0182-17.2017 (2017).

18. Busch, N. A., Dubois, J. & VanRullen, R. The phase of ongoing EEG oscillations predicts visual perception. *J. Neurosci.* **29**, 7869–7876 (2009).

19. Wimmer, K. *et al.* Transitions between multiband oscillatory patterns characterize memory-guided perceptual decisions in prefrontal circuits. *J. Neurosci.* **36**, 489–505 (2016).

20. Samaha, J., Iemi, L. & Postle, B. R. Prestimulus alpha-band power biases visual discrimination confidence, but not accuracy. *Conscious. Cogn.* **54**, 47–55 (2017).

21. Samaha, J., Switzky, M. & Postle, B. R. Confidence boosts serial dependence in orientation estimation. *J. Vis.* **19**, 25 (2019).

22. Samaha, J., Iemi, L., Haegens, S. & Busch, N. A. Spontaneous Brain Oscillations and Perceptual Decision-Making. *Trends Cogn. Sci.* **24**, 639–653 (2020).

23. Pinto, L., Tank, D. W. & Brody, C. D. Multiple timescales of sensory-evidence accumulation across the dorsal cortex. *eLife* **11**, e70263 (2022).

24. Soltani, A., Murray, J. D., Seo, H. & Lee, D. Timescales of cognition in the brain. *Curr. Opin. Behav. Sci.* **41**, 30–37 (2021).

25. Wang, H., Stradtman, G. G., Wang, X.-J. & Gao, W.-J. A specialized NMDA receptor function in layer 5 recurrent microcircuitry of the adult rat prefrontal cortex. *Proc. Natl. Acad. Sci. U. S. A.* **105**, 16791–16796 (2008).

26. Deco, G. & Romo, R. The role of fluctuations in perception. *Trends Neurosci.* **31**, 591–598 (2008).

27. Roach, J. P., Churchland, A. K. & Engel, T. A. Choice selective inhibition drives stability and competition in decision circuits. *Nat. Commun.* **14**, 147 (2023).

28. Schmidt, H., Avitabile, D., Montbrió, E. & Roxin, A. Network mechanisms underlying the role of oscillations in cognitive tasks. *PLOS Comput. Biol.* **14**, e1006430 (2018).

29. Youssofzadeh, V., Prasad, G. & Wong-Lin, K. On self-feedback connectivity in neural mass models applied to event-related potentials. *NeuroImage* **108**, 364–376 (2015).

30. Wong, K.-F. & Wang, X.-J. A recurrent network mechanism of time integration in perceptual decisions. *J. Neurosci. Off. J. Soc. Neurosci.* **26**, 1314–1328 (2006).

31. Wilson, H. R. & Cowan, J. D. Excitatory and Inhibitory Interactions in Localized Populations of Model Neurons. *Biophys. J.* **12**, 1–24 (1972).

32. Roach, S. M. *et al.* A cortical circuit mechanism for encoding decision confidence. *Nat. Neurosci.* **26**, 85–95 (2023).

33. Najafi, F. *et al.* Excitatory and Inhibitory Subnetworks Are Equally Selective during Decision-Making and Emerge Simultaneously during Learning. *Neuron* **105**, 165-179.e8 (2020).

34. Gerstner, W., Kistler, W. M., Naud, R. & Paninski, L. *Neuronal Dynamics: From Single Neurons to Networks and Models of Cognition*. (Cambridge University Press, 2014).

35. *Dynamic-Clamp: From Principles to Applications*. (Springer US, New York, NY, 2009). doi:10.1007/978-0-387-89279-5.

36. Kepecs, A., Uchida, N., Zariwala, H. A. & Mainen, Z. Neural correlates, computation and behavioural impact of decision confidence. *Nature* **455**, 227–231 (2008).

37. Vugt, M. K. van, Simen, P., Nystrom, L., Holmes, P. & Cohen, J. Lateralized Readiness Potentials Reveal Properties of a Neural Mechanism for Implementing a Decision Threshold. *PLoS ONE* **9**, (2014).

38. Atiya, N. A. A., Rañó, I., Prasad, G. & Wong-Lin, K. A neural circuit model of decision uncertainty and change-of-mind. *Nat. Commun.* **10**, 2287 (2019).

39. Shadlen, M. N. & Newsome, W. T. Neural basis of a perceptual decision in the parietal cortex (area LIP) of the rhesus monkey. *J. Neurophysiol.* **86**, 1916–1936 (2001).

40. Shadlen, M. N. & Newsome, W. T. Neural Basis of a Perceptual Decision in the Parietal Cortex (Area LIP) of the Rhesus Monkey. *J. Neurophysiol.* **86**, 1916–1936 (2001).

41. Roitman, J. D. & Shadlen, M. N. Response of neurons in the lateral intraparietal area during a combined visual discrimination reaction time task. *J. Neurosci. Off. J. Soc. Neurosci.* **22**, 9475–9489 (2002).

42. Wang, X.-J. Probabilistic decision making by slow reverberation in cortical circuits. *Neuron* **36**, 955–968 (2002).

43. Sanchez Bornot, J. M., Wong-Lin, K., Ahmad, A. L. & Prasad, G. Robust EEG/MEG Based Functional Connectivity with the Envelope of the Imaginary Coherence: Sensor Space Analysis. *Brain Topogr.* **31**, 895–916 (2018).

44. Wong, K.-F., Huk, A. C., Shadlen, M. N. & Wang, X.-J. Neural circuit dynamics underlying accumulation of time-varying evidence during perceptual decision making. *Front. Comput. Neurosci.* **1**, (2007).

45. Buzsáki, G. & Wang, X.-J. Mechanisms of gamma oscillations. *Annu. Rev. Neurosci.* **35**, 203–225 (2012).

46. Moran, R. J. *et al.* Dynamic causal models and physiological inference: A validation study using isoflurane anaesthesia in rodents. *PLoS ONE* **6**, e22790 (2011).

47. Ratcliff, R. & McKoon, G. The diffusion decision model: theory and data for two-choice decision tasks. *Neural Comput.* **20**, 873–922 (2008).

48. Voytek, B. *et al.* Age-Related Changes in 1/f Neural Electrophysiological Noise. *J. Neurosci.* **35**, 13257–13265 (2015).

49. Friston, K. J. Hierarchical models in the brain. *PLoS Comput. Biol.* **4**, e1000211 (2008).

50. Destexhe, A., Rudolph, M., Fellous, J.-M. & Sejnowski, T. J. Fluctuating synaptic conductances recreate in vivo-like activity in neocortical neurons. *Neuroscience* **107**, 13–24 (2001).

51. Buzs'aki, G. & Draguhn, A. Neuronal oscillations in cortical networks. *Science* **304**, 1926–1929 (2004).

52. Ermentrout, B. ,. Author & Mahajan, A. ,. Reviewer. Simulating, Analyzing, and Animating Dynamical Systems: A Guide to XPPAUT for Researchers and Students. *Appl. Mech. Rev.* **56**, B53 (2003).